



HAL
open science

Influence of medium viscosity on the heating power and the high-frequency magnetic properties of nanobeads containing magnetic nanoparticles

A. Rousseau, M. Tellier, L. Marin, M. Garrow, C. Madelaine, N. Hallali, J. Carrey

► To cite this version:

A. Rousseau, M. Tellier, L. Marin, M. Garrow, C. Madelaine, et al.. Influence of medium viscosity on the heating power and the high-frequency magnetic properties of nanobeads containing magnetic nanoparticles. *Journal of Magnetism and Magnetic Materials*, 2021, 518, pp.167403 -. 10.1016/j.jmmm.2020.167403 . hal-03493710

HAL Id: hal-03493710

<https://hal.science/hal-03493710>

Submitted on 17 Oct 2022

HAL is a multi-disciplinary open access archive for the deposit and dissemination of scientific research documents, whether they are published or not. The documents may come from teaching and research institutions in France or abroad, or from public or private research centers.

L'archive ouverte pluridisciplinaire **HAL**, est destinée au dépôt et à la diffusion de documents scientifiques de niveau recherche, publiés ou non, émanant des établissements d'enseignement et de recherche français ou étrangers, des laboratoires publics ou privés.



Distributed under a Creative Commons Attribution - NonCommercial 4.0 International License

Influence of medium viscosity on the heating power and the high-frequency magnetic properties of nanobeads containing magnetic nanoparticles

A. Rousseau^{*,1}, M. Tellier^{*,1}, L. Marin^{*,1}, M. Garrow^{*,1}, C. Madelaine¹, N. Hallali² and J. Carrey²

* Equal contribution

E-mail adress : julian.carrey@insa-toulouse.fr

¹ Lycée Polyvalent Marie-Louise Dissard Françoise, 5 Boulevard Alain Savary, F-31170, Tournefeuille, France

² Université de Toulouse; INSA; UPS; LPCNO (Laboratoire de Physique et Chimie des Nano-Objets), 135 avenue de Ranguel, F-31077 Toulouse, France

ABSTRACT

Magnetic nanoparticles placed in a high frequency alternating magnetic field release heat. This phenomenon can be used to heat and kill cancerous cells, the so-called magnetic hyperthermia treatment. Our study focuses on the influence of the medium viscosity on the heating power of magnetic nanobeads (MNBs) containing superparamagnetic nanoparticles. The specific absorption rate (SAR) of two types of MNBs differing by their size was determined by measuring the area of their high-frequency hysteresis loops. Three different behaviors are observed as viscosity rises: (i) SAR first drops to a minimum value for both MNB sizes; (ii) interestingly, and only for smaller MNBs, after going through a minimum, SAR increases again towards a steady

value; (iii) for larger MNBs, SAR remains constant after reaching its minimum value. The physical origin of these different behaviors is interpreted, the key ingredient to explain them being the magnetic interactions, the possibility of the bead to form chains, and their possibility to physically rotate under the influence of the magnetic field. Finally these results lead to questioning the representativeness of SAR measurements in water for nanoparticles intended for biological applications, in which the medium viscosity is very different from the one of water.

INTRODUCTION

In 1957, Gilchrist R.K. *et al.* [1] proposed a novel antitumor treatment consisting in the injection of iron oxide nanoparticles directly inside tumors. Then, by applying a high-frequency alternating magnetic field (AMF), nanoparticles heated because of hysteresis losses and destructed tumoral cells. That was the beginning of magnetic hyperthermia approach. Another promising approach called “targeted magnetic intra-lysosomal hyperthermia” might solve some drawbacks of the conventional method. In this new approach, nanoparticles are grafted with specific ligands corresponding to the receptors overexpressed in cancerous cells; they only penetrate targeted cells and accumulate in their lysosomes. The heat released when AMF is applied then induces lysosomal membrane permeabilization, releasing toxic enzymes and leading to a non-apoptotic death of the targeted cell [2,3].

A part of research in this field focuses on the synthesis of biocompatible magnetic nanoparticles (MNPs) with the largest heating power, called Specific Absorption Rate (SAR), which is often determined by measuring the properties of nanoparticles suspended in water. However, MNP heating power does not only depend on their own characteristics but also on the physicochemical

properties of the environment they are placed in. Human body and lysosomes in particular are media with a high viscosity [4,5]. Several reports have shown that the environment viscosity has a non-negligible impact on the MNP heating power [6,7,8,9,10]. Therefore, the representativeness of heating power measurements in water can be questioned for biomedical applications. In Ref.[7] SAR values of single core MNPs and multicores MNPs, known as magnetic nanobeads (MNBs) were measured inside different viscous fluids. Results indicate a SAR decrease when viscosity rises for single or multi-core MNPs. Similar results were also obtained in Refs.[6,10].

The research presented in this paper is focused on the influence of the viscosity of the surrounding medium on the SAR of two batches of MNBs, which differ only by their diameter. We found results similar to the ones cited above for our large MNBs but for small ones, we surprisingly observed an additional rise of SAR value when agarose content, and therefore viscosity, increases. Furthermore, our high frequency hysteresis loop measurement setup allowed us to observe MNB magnetic properties dependence on viscosity. Some interpretations based on these observations and on literature are provided to explain the differences in the magnetic and heating properties of these two batches.

METHODOLOGY

a. Materials

The studied MNPs are two batches of FluidMag-PEG/Amine (Chemicell, Germany) with different diameters: 100 nm and 200 nm. They are composed of several magnetic cores clustered and coated by a shell of PEG-amine, as shown schematically in Fig.1a. According to manufacturer (datasheet and personal communication), whatever the hydrodynamic diameter of the beads, magnetic cores are composed of a cluster of iron oxide NPs (Fe_3O_4) embedded in a

polymer matrix (PEG – 20 000 Da), and amine molecules as functional group. The nominal size of the cores is around 10 nm and the beads contain 1.25 g Fe₃O₄/cm³, which corresponds to a mean volume concentration of Fe₃O₄ inside the bead of approximately 24%. The cluster has a mean size of 75 nm and 175 nm for batches containing MNBs with a diameter of 100 nm (MNBs-100) and 200 nm (MNBs-200), respectively [see Fig. 1(a)]. This means that the volume concentration of the MNPs inside the cluster is larger than the estimate provided above since the MNPs are concentrated inside the cluster and not dispersed evenly inside the bead.

To vary sample viscosity, agarose powder (Eurobio, France) was mixed at different percentage weight per volume (from 0.1%w/v to 10%w/v) with hot water (at 90°C) to form stock solutions. Then 0.25 mL of each stock solution was injected inside glass tubes and completed with 0.25 mL of one of the MNB solutions. Thus, the final agarose content inside each tube was twice as low compared to stock solutions. Finally, each sample was sonicated, placed in a fridge at 4°C during 48 hours before use to ensure a stabilization of the agarose gel mechanical properties, as explained in Ref.[11].

The agarose percentage range used was chosen because it frames viscosity values, which MNBs can be exposed to when they are used for biological applications. For example, 2.5% of agarose content can mimic mechanical properties of soft tissues [18] with an estimated viscosity around 100 Pa.s [11]. Also, here are viscosity values measured inside different biological medium: 50 to 90 mPa.s inside lysosomes [12], 4 mPa.s for cytoplasm [4], and several hundred of Pa.s for cancer cells [13]. To compare, viscosity of water is 1 mPa.s.

b. TEM measurement

Samples for TEM analysis were prepared by deposition of a drop of a diluted solution on an amorphous carbon-coated copper grid. Low-resolution images were obtained using a JEOL-1400 microscope operating at 120 kV.

c. Magnetic measurements

Magnetic measurements were performed using a vibrating sample magnetometer (VSM) (PPMS – Quantum Design). Inside a VSM capsule 5 μ L of MNBs solution were deposited and left 24 hours in the open air to obtain dry MNBs. The capsule was then sealed and hysteresis loops were performed in a -5/+5 T range at 300 K.

d. High-frequency hysteresis loop measurements

High-frequency hysteresis loop measurements were performed using a home-made coil, described in Ref.[14] and generating an AMF with an amplitude of 35 mT at 50 kHz. Magnetic field was applied during 60s and hysteresis loops were collected during this period of time.

Coercive field (H_c), magnetic susceptibility (χ) and SAR values were determined from hysteresis loop measurements. SAR is expressed in watt per gram of iron oxide, and is calculated by multiplying the hysteresis loop area of the sample by the magnetic field frequency (50.31 kHz for MNBs-100 and 50.43 kHz for MNBs-200). Magnetic susceptibility is dimensionless and is obtained by calculating the derivative of the hysteresis loop in the vicinity of H_c .

As mentioned in Ref.[14], measured hysteresis loops depend on the homogeneity of the magnetic material over the entire height of the sample. Because MNBs-200 are large particles, they tend to sediment and their concentration along the height of the sample can be different. To quantify this variation, hysteresis loops of each sample containing MNBs-200 were measured at two different heights, then the mean and standard deviation of the measurements were calculated.

RESULTS

According to the TEM observation performed on MNBs-100, the size of magnetic cores varies from 5 to 30 nm [see Fig.1(b)]. Magnetic core sizes for MNBs-200 is expected to be the same than for MNBs-100 according to the manufacturer. This core size is consistent with the superparamagnetic behavior measured by VSM at 300 K for both MNBs-100 and MNBs-200 [see Fig.1(c)]. These measurements were achieved directly on stock solutions and allowed us to estimate their iron oxide concentration by dividing the measured saturated magnetization by the specific magnetization of bulk Fe_3O_4 , which is 85 A.m²/kg. The iron oxide concentration for MNBs-100 and MNBs-200 was respectively 16 mg Fe_3O_4 / mL and 22 mg Fe_3O_4 / mL. Since the magnetization of the particles is probably lower, these values should be considered as lower bounds.

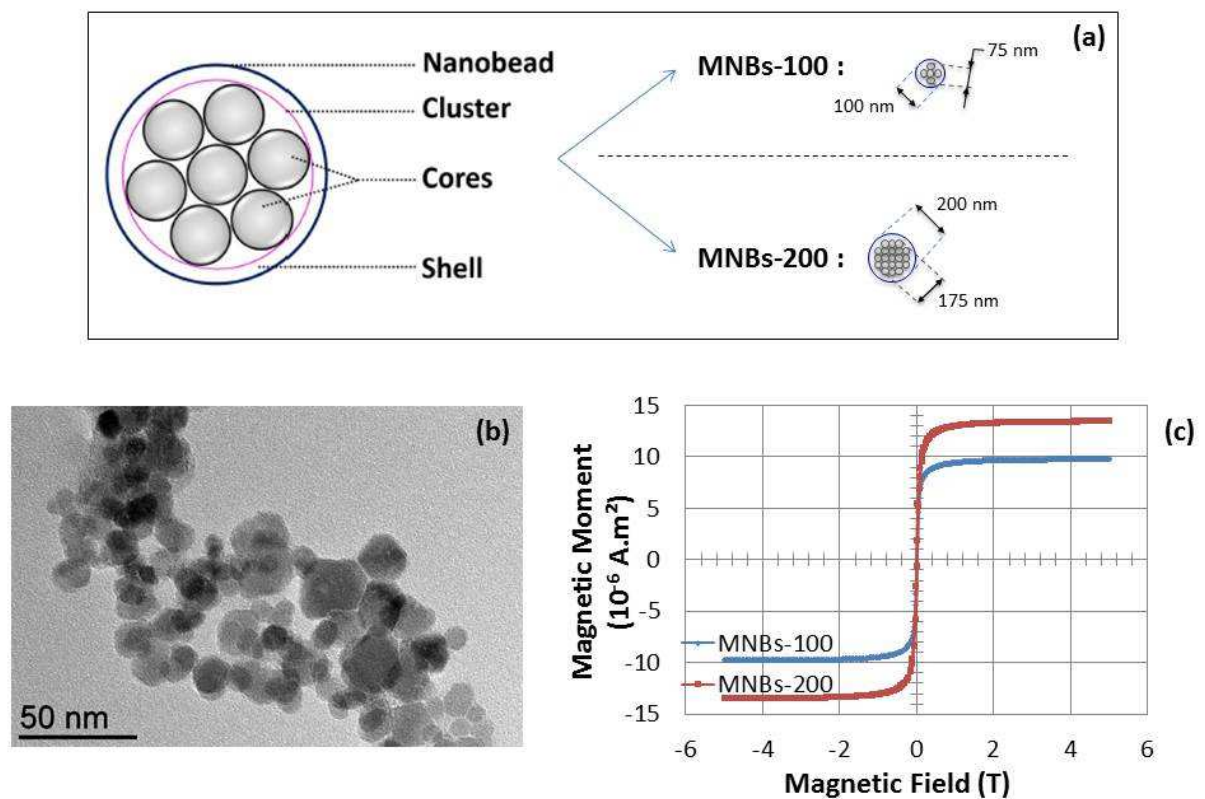


Fig.1: Description of MNBs used. (a) Schematic representation of MNBs, according to datasheet and personal communication provided by manufacturer of these MNBs as mentioned in “methodology” section, part (a). (b) TEM picture of MNPs inside MNBs-100. (c) VSM measurements on MNBs-100 and MNBs-200 at 300 K.

To measure the impact of viscosity on MNB magnetic properties, several samples were prepared containing one type of MNBs (MNBs-100 or MNBs-200) in a known concentration of agarose. It is expected that the higher the agarose concentration, the higher the viscosity. The agarose percentage ranged from 0.05% to 2.5%. Then samples were placed inside a high-frequency magnetometer and their hysteresis loop was measured at 50 kHz. This magnetometer is a home-

made setup described in the “methodology” section, part (d) and detailed in Ref.[14]. We chose this method to measure SAR instead of temperature measurements (calorimetric method) because we suspect that different gelling state of the samples could induce different thermal conductivities into the sample, as well as between the samples and the calorimeter, because of the absence or slowdown of convection. As a consequence, it could have been argued that an observed difference in the SAR of the different samples could originate from different thermal diffusion and not from changes in the viscosity itself. Magnetic estimation of SAR removes this possible artefact. Measurements started with a temperature around 21°C, and ended at a maximum of 27°C because of the MNB heating (curves not shown). The gelling temperature of agarose is around 37°C and, as shown in Ref.[15], when temperature of agarose is below this value, its mechanical properties do not change significantly. Thus, even if the temperature increased by at most 6°C, we assume that, during each measurement, the mechanical properties of the samples do not vary.

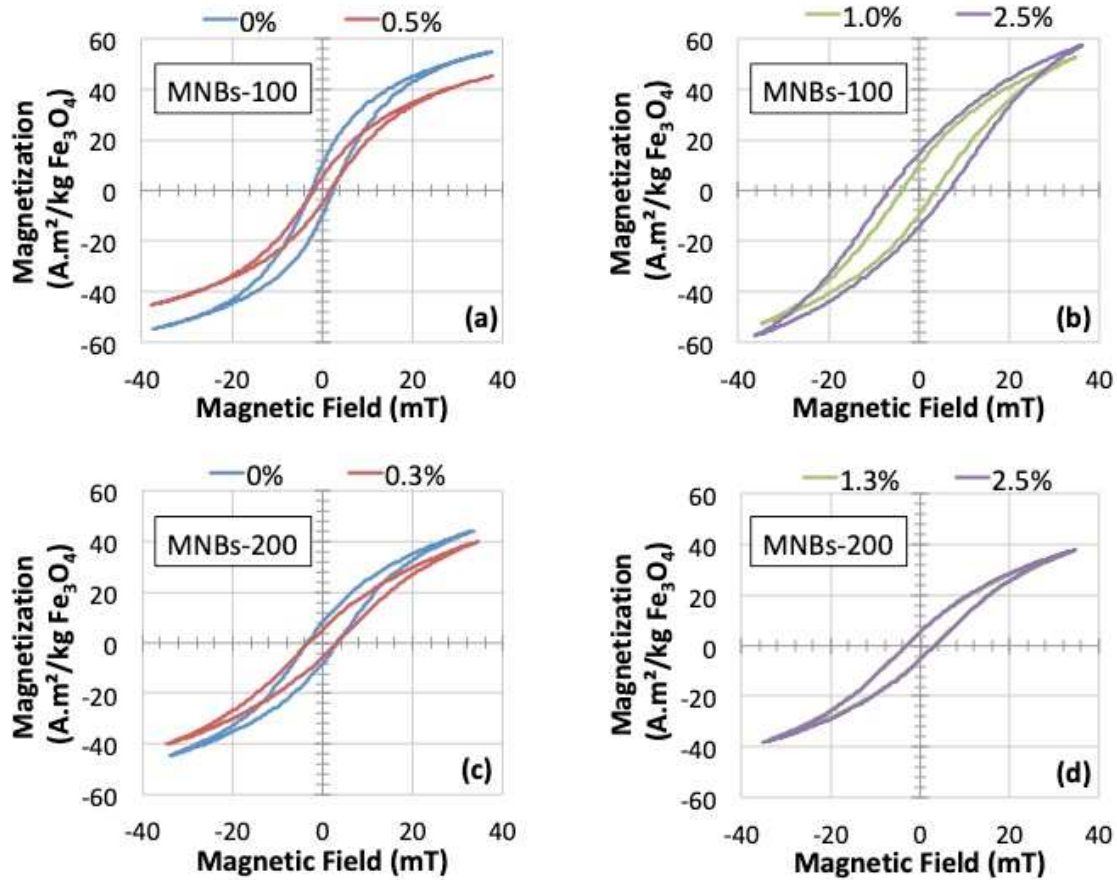


Fig.2: High-frequency hysteresis loops measured on MNBs, for different values of agarose concentration, using an AMF of 50 kHz and 35 mT. (a) and (b) MNBs-100 with agarose content of 0%, 0.5%, 1% and 2.5%. (c) and (d) MNBs-200 with agarose content of 0%, 0.3%, 1.3% and 2.5%. These last two concentrations (1.3% and 2.5%) present similar hysteresis loop and thus their data points are superimposed.

High-frequency hysteresis loops of both MNBs at different agarose concentrations are presented in Fig.2. In Fig.2(d) hysteresis loops of MNBs-200 with agarose content of 1.3% and 2.5% are indistinguishable from each other. To evaluate more precisely the influence of the agarose content on magnetic properties of MNBs, magnetic susceptibility (χ), and coercive field (H_c)

were picked up for each sample and plotted (see Fig.3). To describe these results, two ranges of agarose concentration will be distinguished, the “low viscosity” and the “high viscosity”, which correspond respectively to values from 0% to 0.3% and from 0.3% to 2.5% for MNBs-200 (or from 0% to 0.5% and from 0.5% to 2.5% for MNBs-100). Although the exact agarose concentration values are different for the two series of samples, they are contained inside the same concentration range (0% to 2.5%) and allow comparing evolution of their magnetic properties.

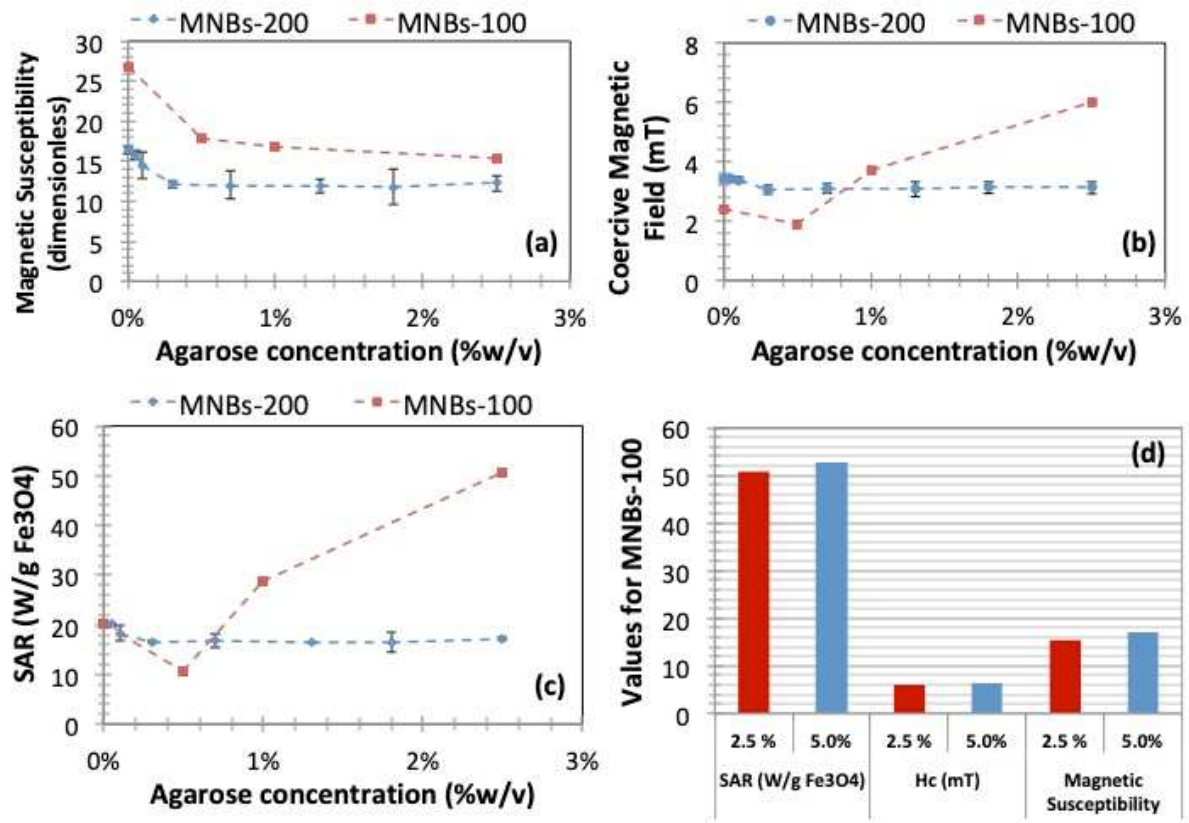


Fig.3: Magnetic properties of MNBs, picked up or calculated from their high-frequency hysteresis loops. (a) Magnetic susceptibility, (b) coercive field, and (c) SAR are plotted for

MNBs-100 and MNBs-200 as a function of agarose concentration. (d) Values of SAR, H_c and magnetic susceptibility at 2.5% and 5% of agarose concentration for MNBs-100.

In Fig.3(a), magnetic susceptibility of MNBs is plotted as a function of agarose concentration. At 0% of agarose content, MNBs-100 have a higher magnetic susceptibility ($\chi = 26.8$) than MNBs-200 ($\chi = 16.4$). For both type of MNBs, it strongly decreases in the « low viscosity » regime. In the « high viscosity » regime, susceptibility slowly decreases for MNBs-100 until a value about 15.4 at 2.5%. For MNBs-200 a steady value of magnetic susceptibility, around 12.0, is reached from 0.3% onwards. In Fig.3(b), H_c at 0% is higher for MNBs-200 (3.5 mT) than for MNBs-100 (2.4 mT). Then a drop of its value is observed for both MNBs for « low viscosity » even if this is more important for MNBs-100 than for MNBs-200. For the bigger MNBs, H_c reaches a steady value of 3 mT for « high viscosity », whereas for smaller ones H_c increases from 1.9 mT to 6 mT at 2.5%. The SAR for the two samples varies in the same way as H_c [see Fig.3(c)]. Finally, it can be noted that MNBs-100 were also characterized within a viscous medium containing 5% of agarose concentration; their high-frequency hysteresis loop was exactly the same than for 2.5% [see Fig.3(d)].

DISCUSSION

In this part the origin of SAR variations as a function of agarose content is discussed. Because SAR variations are identical to H_c variations, for both types of MNBs, we will focus on H_c as main cause of SAR evolution. In our interpretation, which is summarized in Fig.4, these variations result from changes in the MNB mobility and spatial organization. MNBs-200 follow two regimes: “chains” at low viscosity and “immobility” for high viscosity, while MNBs-100

follow three regimes: “chains” for low viscosity, “partial rotations” for intermediate viscosity and “immobility” for high viscosity. These different regimes are discussed below.

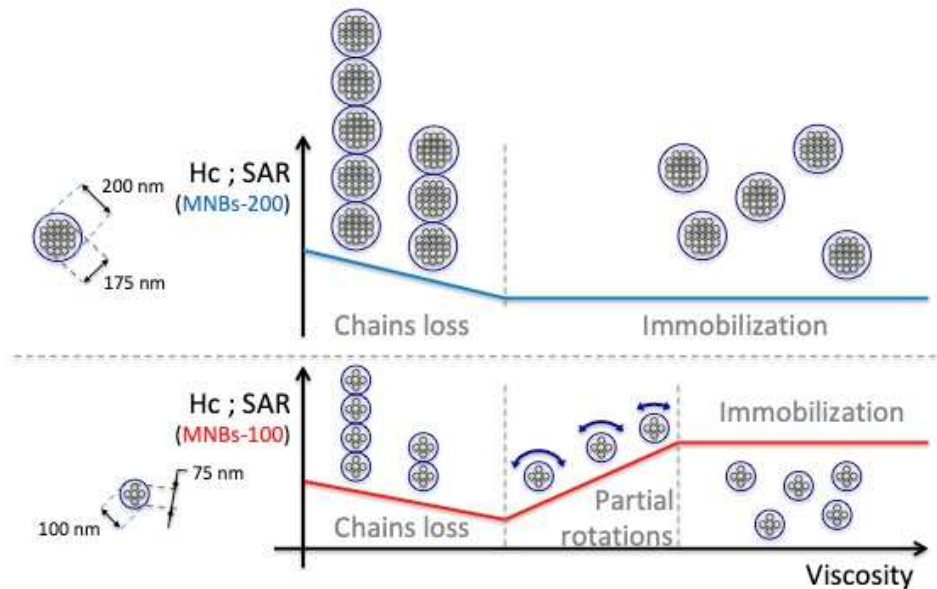


Fig.4: Schematic of the different behaviors of MNBs-100 and MNBs-200 as a function of the viscosity.

At high viscosity, for concentration larger than 2.5%, MNBs-200 and MNBs-100 can be considered as immobilized particles as their magnetic properties (magnetic susceptibility, coercive field and SAR) do not vary with an increase of viscosity. In a sense, at high viscosity, our measurements reveal the intrinsic properties of the beads. We interpret the fact that the MNBs-100 display a coercive field value larger than the MNBs-200 as resulting from the magnetic interactions between the MNPs inside the bead. Indeed, let us recall that the size of the MNPs inside the bead is quite small and that these particles, if they were measured individually, would certainly display a clear superparamagnetic behavior, with a null or negligible coercive field. The presence of a non-null coercive field is thus very likely to be extrinsic and to originate

from the interactions between the MNPs, as shown in, for instance, Ref.[16]. For large volume concentrations as the ones of the clusters of MNPs inside the beads (see above), the coercive field decreases with the size of the beads, as illustrated in the Fig.5(c) and Fig.10 of Ref.[16]. Thus we interpret the decrease of coercive field in MNBs-200 compared to MNBs-100 as resulting from an increase of magnetic interactions in an assembly of compact superparamagnetic MNPs. This interpretation would also explain the lower value of magnetic susceptibility for MNBs-200, whatever the agarose content, than for MNBs-100.

At low viscosity, for agar concentration values below 0.2-0.5%, both MNBs-100 and MNBs-200 see their H_c and SAR values rise as the agarose concentration (i.e. the viscosity) decrease. This increase is also associated with a gain of magnetic susceptibility, which can be explained by the capacity of MNBs to form chains. Indeed, as explained in Refs.[17,18,19,20,21], when MNPs have the possibility to arrange themselves to form chains, the global magnetic susceptibility as well as the SAR value rise (see « Chains» in Fig.4 for an illustration). An increase of H_c in randomly oriented MNPs arranged in chains has also been shown in Refs.[21,21]. Although one has to be cautious on this point, data seem to indicate a stronger effect of the chain formation on MNBs-100 than on MNBs-200. At least two phenomena could be at the origin of this effect: chains could be formed faster or could be more anisotropic once formed. Indeed, results from our group show that, in some cases, the time scale on which these chains form is of the order of minutes, even in low-viscosity solvents [22]. Here, hysteresis loop measurements were obtained 60 seconds after the field has been switched on; it is possible that the chains, especially for low viscosities, had not completely achieved their formation when the sample properties were measured: MNBs-200 being larger, it could be possible that their dynamic is slower.

Between 0.5% and 2.5% of agarose concentration, MNBs-100 specifically show a regime which is not observed in MNBs-200, and is illustrated as «partial rotations» in Fig.4. This regime is characterized by a significant decrease of both SAR and coercive field, while the susceptibility increases slightly. We interpret this behavior as the sign that, in this intermediate range of viscosities, the MNBs have the possibility and time to rotate under the influence of the torque generated by the magnetic field application, and align their “global” anisotropy axes with the magnetic field, which is indeed expected to lead to a decrease of coercive field and an increase of susceptibility (see, e.g. Fig.7 of Ref.[23]). Naturally, the lower the viscosity, the faster the partial rotation is expected to occur, and so the smaller the coercive field. The fact that this “partial rotations” regime is not observed for the MNBs-200 could come from their larger size, although it is not obvious to demonstrate it, since increasing the size of the bead increases at the same time the force acting to rotate the bead and the shear force. Finally, according to our model, increase the frequency of the magnetic field would influence the “partial rotation” regime by stopping MNBs motion for lower viscosity value. This would be consistent with the fact that the Brown relaxation becomes negligible face to Néel relaxation as frequency increases.

CONCLUSION

This study shows that the heating power of magnetic nanobeads greatly depends on the environment viscosity and on the size of the nanobeads. Different behaviors were observed on magnetic nanobead batches which only differ by their cluster size and hydrodynamic diameter. In particular, the MNBs-100 sample presented three different regimes, which have been interpreted using data from the literature. Both investigated nanobead batches experience a clear SAR drop for low viscosities. Then, as viscosity rises, the SAR of smaller nanobeads rises again whereas

the one of larger nanobeads remains constant and is then somehow independent of environment viscosity. As biological tissues are viscous environments, our observations confirm that SAR measurements carried out in water are not relevant when they are intended to biological applications.

Then, as far as the use of magnetic nanobeads in targeted intra-lysosomal hyperthermia is concerned, these results could prove very useful. Indeed, if lysosomal viscosity value is beyond the ones corresponding to the SAR drop, adjusting magnetic nanobead sizes so that they behave like the larger nanobeads batch could overcome the viscosity related issues so the heating power would no longer depend on the local viscosity values and on their variation once there are internalized inside the cells.

ACKNOWLEDGMENT

We thank Lise-Marie Lacroix, Arnaud Hillion and Nicolas Mille for their support respectively on TEM, VSM and high frequency hysteresis loop measurements. We also thank Véronique Gigoux for fruitful discussions on the choice of the gelling agent used.

References:

- [1] R.K. Gilchrist, R. Medal, W.D. Shorey, R.C. Hanselman, J.C. Parrott, C.B. Talor. *Ann. Surg.* **146**. 596 (1957)
- [2] C. Sanchez, D. El Hajj Diab, V. Connord, P. Clerc, E. Meunier, B. Pipy, B. Payré, R.P. Tan, M. Gougeon, J. Carrey, V. Gigoux, and D. Foumy. *ACS Nano*. **8**, 1350. (2014)
- [3] P. Clerc, P. Jeanjean, N. Hallali, M. Gougeon, B. Pipy, J. Carrey, D. Fourmy, V. Gigoux. *J. Cont. Rel.* **270**. 120 (2018)
- [4] A.L. Urbano-Bojorge, O. Casanova-Carvajal, N. Félix-González, L. Fernández, R. Madurga, S. Sánchez-Cabezas, E. Aznar, M. Ramos, and J.J. Serrano-Olmedo. *Nanotechn.* **29**. 385705 (2018)
- [5] L.E. Shimolina, M.A. Izquierdo, I. Lopez-Duarte, J.A. Bull, M.V. Shirmanova, L.G. Klapshina, E.V. Zagaynova, and M.K. Kuimova. *Sci. Rep.* **7**. 41097 (2017)
- [6] N.A. Usov, and B.Ya. Liubimov. *J. App. Phys.* **112**. 023901 (2012)
- [7] R. Ludwig, M. Stapf, S. Dutz, R. Müller, U. Teichgräber, and I. Hilger. *Nanoscale Res. Lett.* **9**. 602 (2014)
- [8] S. Dutz, M. Kettering, I. Hilger, R. Müller, and M. Zeisberger. *Nanotechn.* **22**. 265102 (2011)
- [9] C. Guibert. Etude des propriétés d'hyperthermie de nanoparticules dispersées dans des systèmes complexes. UPMC. PHENIX (2015).
- [10] D. Cabrera, J. Camarero, D. Ortega, F.J. Teran. *J. Nanopart. Res.* **17**. 121 (2015)
- [11] A.L. Ellis, A.B. Norton, T.B. Mills, I.T. Norton. *Food Hydrocolloids*. **73**. 222 (2017)
- [12] L. Wang, Y. Xiao, W. Tian, and L. Deng. *J. Am. Chem. Soc.* **135**. 2903 (2013)
- [13] C. Rianna, M. Radmacher. *Eur. Biophys. J.* **46**. 309 (2017)
- [14] V. Connord, B. Mehdaoui, R. P. Tan, J. Carrey, M. Respaud, *Rev. Sci. Instrum.* **85**. 093904 (2014)
- [15] B. Mao, T. Divoux, and P. Snabre. *J. of Rheo.* **60**. 473 (2016)
- [16] R.P. Tan, J. Carrey, and M. Respaud. *PRB*. **90**. 214421 (2014)
- [17] B. Mehdaoui, R.P. Tan, A. Meffre, J. Carrey, S. Lachaize, B. Chaudret, and M. Respaud. *PRB*. **87**. 174419 (2013)

-
- [18] E. Myrovali, N. Maniotis, A. Makridis, A. Terzopoulou, V. Ntomprougkidis, K. Simeonidis, D. Sakellari, O. Kalogirou, T. Samaras, R. Salikhov, M. Spasova, M. Farle, U. Wiedwald, and M. Angelakeris. *Sci. Rep.* **6**. 37934 (2016)
- [19] S. L. Saville, B. Qi, J. Baker, R. Stone, R. E. Camley, K. L. Livesey, L. Ye, T. M. Crawford, O. T. Mefford. *J. Col. and Int. Scie.* **424**. 141-151 (2014)
- [20] D. Toulemon, M.V. Rastei, D. Schmool, J.S. Garitaonandia, L. Lezama, X. Cattoën, S. Béguin-Colin, and B.P. Pichon. *Adv. Func. Mat.* **26**. 2454 (2016)
- [21] D. Serantes, K. Simeonidis, M. Angelakeris, O. Chubykalo-Fesenko, M. Marciello, M. del Puerto Morales, D. Baldomir, and C. Martinez-Boubeta. *J. of Phy. Chem. C.* **118**. 5927 (2014)
- [22] N. Mille *et al.* in preparation.
- [23] H. Mamiya and B. Jeyadevan, *Scientific Reports* **1**, 157 (2011).